Philosophical Magazine,
Vol. 86, Nos. 33–35, 21 Nov.–11 Dec. 2006, 5383–5396

Taylor & Francis
Taylor & Francis Group

Strength measurement of a brittle coating with a trilayer structure using instrumented indentation and *in situ* observation techniques

J. H. KIM†, H.-K. LEE† and D. K. KIM*†

†Department of Materials Science and Engineering, Korea Advanced Institute of Science and Technology (KAIST), Kusong-Dong, Yusong-Gu, Daejeon 305-701, South Korea

(*Received 15 November 2005; in final form 18 April 2006*)

A mechanical-testing method, devised to measure the strength of brittle thin coatings with a trilayer structure, was investigated. A semi-empirical relationship among radial cracking and associated parameters was derived by introducing a buffer and coating layer with an effective thickness concept, extending the established bilayer equation. Adjustable parameters of the proposed trilayer equation were determined for various ratios of coating thicknesses and moduli. The validity of the FEA-based relationship was analyzed by an experimental method utilizing a graphite/glass/substrate structure. An *in situ* observation of radial cracks through the transparent substrate during sphere indentation enabled the determination of the strength of the thin coating layer. Chemical vapour-deposited silicon carbide films were used to evaluate the strength and Weibull modulus using the present technique, in a case study format. The validity of the trilayer equation in terms of critical load for radial cracking and the strength of the thin brittle coating are discussed. This study can contribute to knowledge in the area of evaluating brittle thin coating systems on a compliant substrate.

1. Introduction

Brittle coatings are utilized in a wide range of engineering applications, such as thermal barrier coatings [1], cutting tools [2], car windshields, dental restoration [3] and protective coatings in nuclear fuel (TRISO fuel particles) for next-generation gas-cooled nuclear reactors [4]. Owing to their high strength and hardness, chemical inertness, and high temperature stability, they inhibit the failure of important components in engineering applications by absorbing and confining external contact damage [5]. Generally, brittle coatings have a tolerance for wear and concentrated external loads, but are occasionally subjected to flexure stress with a soft substrate. When this happens, star-shaped radial cracks are induced on the bottom surface of the brittle layer, which leads to a rapid loss of function and ultimate failure of the coating structure [6]. To prevent these kinds of fractures, the strength of a brittle

*Corresponding author. Email: dkkim@kaist.ac.kr

Philosophical Magazine
ISSN 1478–6435 print/ISSN 1478–6443 online © 2006 Taylor & Francis
http://www.tandf.co.uk/journals
DOI: 10.1080/14786430600796569

coating is considered as the primary factor for determining the relevance of coating systems.

In layered systems, the evaluation of the coating strength is successfully demonstrated by measuring the critical load for radial cracking at the undersurface of brittle coatings [7]. It is well-documented that the critical load for radial cracking in a bilayer structure varies systematically with the coating thickness, the modulus mismatch and the coating strength. Extending this relationship, Miranda *et al*. [8] formulated a methodology for measuring the coating strength theoretically and experimentally by conducting a sphere indentation on glass as well as several ceramic coating systems. Moreover, considering multi-layered systems such as a trilayer structure and an adhesive interlayer [8], semi-empirical and analytical equations dealing with the initiation load for the radial cracking of brittle coating systems have been derived [9].

The aforementioned study considers that the primary failure mode of coating systems is due to radial cracking induced by flexure stress from an external load. However, as the coating thickness is decreased, the flexure stress is diminished while the hoop stress is dominant. As a result, the critical load for radial cracking is not consistent with the bilayer equation [10]. Indeed, other failure modes are also introduced in a thin-coating structure and their analysis has not been fully investigated [11]. The Miranda *et al*. [8] trilayer study reported that radial cracking in a trilayer structure with various coating thicknesses and modulus combinations can be explained by a simple equation. However, their study only considered a thick-coating system; thus, their proposed equation is limited to the strength evaluation of a thick system. Thus, it is necessary to work toward an analysis for failure modes and strength measurements of thin-coating structures.

The purpose of this study is to devise a strength measurement for a thin-film coated trilayer structure by adopting an extension of the bilayer and trilayer equation. First, to provide a theoretical background, the bilayer and previous trilayer equations are reviewed. For an analysis of the trilayer structure containing an outer buffer layer, inner coating and substrate, a numerical calculation (finite element analysis) is utilized to determine the stress distribution at the undersurface of the inner coating layer as a function of the indentation load. A semi-empirical relationship for the effective coating thickness of the buffer layer and inner coating system is derived from the results of a regression fit to finite element analysis data with several different modulus mismatches and thickness ratio configurations. The strength of the inner coating material in the trilayer system is determined by obtaining the stress function at the undersurface coating as a function of the applied load. A graphite/glass/substrate is used as a model system, as the radial cracking of a glass layer has been extensively studied previously. In addition, glass and graphite have a large moduli mismatch so that the effect of the modulus mismatch is apparent. A transparent substrate makes an *in situ* observation possible of radial cracking of the inner coating; therefore, the critical load for radial cracking can be measured. According to the brittle solid fracture criterion, radial cracking initiates and propagates rapidly when tensile stress at the undersurface of the inner coating reaches the strength of the inner coating materials. The strength of glass was determined and compared with biaxial strength test data to validate the trilayer equation. In addition, different grades of silicon carbide film were

characterized using the present trilayer equation in the contexts of the microstructure and strength.

2. Numerical analysis: trilayer structure

In this study, the system has a layered structure and the model structure is axisymmetric. It is assumed that the lateral length of the coating layer is horizontally infinite and that the substrate is thick enough to avoid the substrate dimension effect. The layered structure was pressed by a spherical indenter with an increasing indentation load P. Due to the tensile stress on the undersurface of coating layer, radial cracks were generated. The schematic illustration of the bilayer and trilayer is shown in figure 1a. First, the bilayer and trilayer equation proposed by Lawn *et al.* [12] will be summarized and the acceptable range for applying these equations will be discussed, followed by the development of the trilayer equation for a coated trilayer structure.

2.1. *Bilayer and trilayer equations*

In the bilayer structure, it is considered that the coating layer thickness d is bonded to a compliant substrate. Two major fracture modes are defined in the bilayer system in accordance with the coating thickness range [12]. If the coating thickness is thick, the Hertzian stress field produces a quantity of cone cracking or quasiplastic deformation in the coating layer. In the case of a thin coating system, flexure stress mode is activated as a result of the modulus mismatch between the coating and the substrate. This radial crack is identified as a primary source of a coating failure. Extensive studies have been carried out concerning fracture mechanics of radial cracking modes in multiple types of coating structures [13].

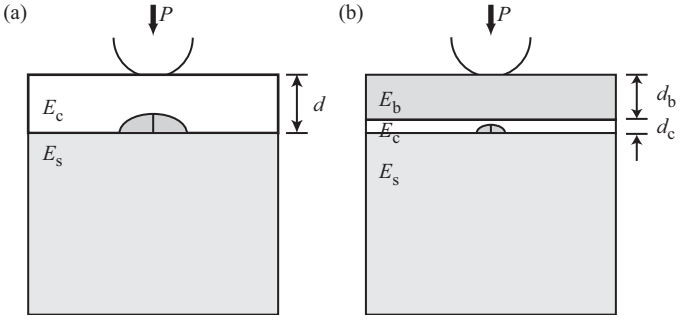

Figure 1. Schematic drawing of the bilayer and trilayer systems. The coating layer of thickness d or d_c, the modulus E_c, buffer of thickness d_b, and the modulus E_b on the coating bonded to the substrate of modulus E_s in contact with the indenting sphere at load P: (a) the coating/substrate bilayer system, (b) the buffer/coating/substrate trilayer system. At the bottom of the coating layer, a trace of a radial crack is indicated.

Under the assumption that the deformation of a substrate remains elastic until a coating failure occurs, the tensile stress on the undersurface of the coating was determined from the theory of plates and shells on an elastic foundation. Equating this relationship, the tensile stress at the coating undersurface can be formulated as follows:

$$\sigma = \frac{P}{Bd^2 \log(E_c/E_s)} \tag{1}$$

where E is the Young's modulus, the subscript c and s denote the coating and the substrate, respectively, and B is a dimensionless correction factor, having a value of 1.8 from the finite element study and experimental results [6]. Critical load measurements enable the determination of the coating strength. The validation of this equation was successfully documented elsewhere and it is not discussed in detail here [6, 10–12]. Equation (1), however, is not valid for thin coating systems because the small contact assumption between indenter and specimen is not true, therefore, the deformation and fracture mechanism of the coating is changed to the complicated mode. This result corresponds to the flaw statistics, the stress state transition, the rate effect, the viscoelasticity, or the cumulative plasticity [12].

Further studies were carried out concerning the trilayer system, as shown in figure 1b. In a previous study, the outer- and inner-layer were considered as an equivalent monolithic coating of thickness $d = d_b + d_c$ and effective modulus E^*. The relationship for the critical load for core radial cracking has a form analogous to:

$$P_R = \frac{B^* \sigma_F d^2}{\log(CE^*/E_s)} \tag{2}$$

where σ_F is the strength of the coating, B^* is the modified coefficient and C is also the correcting factor for trilayer systems determined from finite element analysis [9]. This relationship was tested with indentation experiments on a ceramic trilayer structure and with a finite element analysis. This system is representative of all-ceramic dental crowns with a minimum coating thickness of 0.1 mm. Equation (2) does not describe the radial cracking in thin coating systems, notwithstanding that it integrated two correction factors B^* and C with the effective modulus term E^*. From equations (1) and (2), it is possible to describe the initiation and prevention of cracking in bilayer and trilayer systems; however, any extrapolation of these two equations should be restricted to thick coating systems.

2.2. *Stress analysis and critical load for radial cracking*

Trilayer systems consist of three layers: an outer buffer layer of thickness d_b, an inner coating layer of thickness d_c, and a substrate. The Young's moduli for these are E_b, E_c, and E_s, respectively, as shown in figure 1(b). Generally, in trilayer systems, it is considered that the coating layer has the modulus at the highest level, the buffer layer at an intermediate level, and substrate at the lowest level, i.e. $E_c > E_b > E_s$. The indentation load P with a spherical indenter was applied onto the top surface

of the buffer layer. The purpose of the buffer layer is to increase the total thickness of the coating layer, which in turn enable the extension of the bilayer equation to the trilayer system with a subtle modification. The total thickness remains in an acceptable thickness range of a bilayer by changing the buffer and coating thickness ratio. In this analysis, integrating the effect of the buffer layer thickness and the thickness ratio of the buffer, as well as different moduli conditions into the bilayer equation, was attempted by adding an effective thickness term.

In a simple bilayer system with the coating on a compliant substrate subjected to tensile stress at the bottom surface, which can be described by simple bilayer equation, the buffer layer is introduced on the top of the coating layer and it is assumed that the effective thickness of the coating layer is different from the bilayer relationship. Thus, the thickness term is modified as follows:

$$\sigma = \frac{P \log(E_c/E_s)}{B d_*^2} \tag{3}$$

where B is the same constant and $d_*^2 = d_*(d_b, d_c, E_c/E_b)$, an effective thickness for the coating and buffer layer with the incorporation of each thickness and modulus. The effective thickness term is favoured in this study because the radial cracking in the trilayer structure is reduced to simple bilayer problem. Thus, with known values of the thicknesses and modulus, we can regard a trilayer structure as a simple bilayer one. In equation (3), it is assumed that the coating thickness remains thin, as $d_b/d_c > 10$, and that is has a total thickness larger than 500 μm. The function d_*, which is empirically derived to describe the effective thickness in accordance with the same order of dimension is:

$$d_*^2 = d_b^L \cdot d_c^{2-L} \tag{4}$$

with the dimensionless parameter $L = L(E_c/E_b)$, and with the limiting condition of d_b or $d_c \neq 0$. Empirical functions are used in the present study, since using these is simple and appropriate when describing the effect of the buffer layer. In addition, the form of the function is simple when applying a practical implementation.

To determine the functional dependence of $L = L(E_c/E_b)$, a finite element analysis (FEA, ABAQUS/Standard code) was utilized. All layers and interfaces were assumed to remain fully elastic and well-bonded. An FEA mesh for the trilayer structure and indenting sphere was set as a two-dimensional quadrilateral mesh containing eight nodes. An adaptive mesh was used for the entire system, i.e. the contact and interface regions were fine-meshed and other areas were coarse-meshed. The entire system consisted of approximately 56 000 elements and 55 000 nodes. The system was axisymmetric under the assumption of a semi-infinite lateral distance and substrate thickness. A tungsten carbide sphere of elastic modulus 614 GPa was used to apply a load, which was identical to that in the practical experiments. The fine-meshed interface of the trilayer system reveals a tensile and hoop-stress contour. The contact between the indenting sphere and the trilayer is defined as frictionless. The moduli of the buffer layer and the substrate were fixed at 10 and 2.3 GPa, respectively, from the properties of graphite and polycarbonate.

The modulus of the coating layer varied from 73 to 500 GPa, in the range of known brittle coating systems [14–16]. The total thickness of the coating and buffer layer was fixed at 500 μm, and thickness of the coating layer changed from 5 to 65 μm. In this study, a very thick coating system was not included in the equation, as thick coating systems are well-documented in previous studies [8, 12]. The indentation load increased from zero to several hundreds of N for a sufficient generation of the tensile stress on the bottom surface of the coating layer. The tensile stress on the bottom surface of coating layer varied with the indentation load. The effective thickness parameter $P \cdot \log(E_c/E_s)/(B \cdot \sigma)$ was obtained for each calculation and normalized with the total thickness term. The function d_*/d could be derived from the normalized effective thickness values. The FEA results applied to the simple power law function L as a function of E_b/E_c in figures 2 and 3. The L function can be written as:

$$L = \alpha\left(\frac{E_b}{E_c}\right)^{\beta}. \tag{5}$$

The dimensionless variables α and β are determined from the regression fit of the FEA result to L functions with a numerical iteration. For these values, $\alpha = 1.81$ and $\beta = 0.05$. In figures 2 and 3, the FEA results (data points) and the prediction from the equation (solid curve) are shown as functions of the buffer and coating thickness ratio and the modulus ratio. In the broad thickness and modulus range, the trends of the FEA results are in good agreement with the aforementioned equation.

The trilayer structure can be tested with an indentation experiment. In addition, the strength of the coating layer can be determined by measuring the critical load for radial cracking. Radial crack is generated when tensile stress at the coating layer

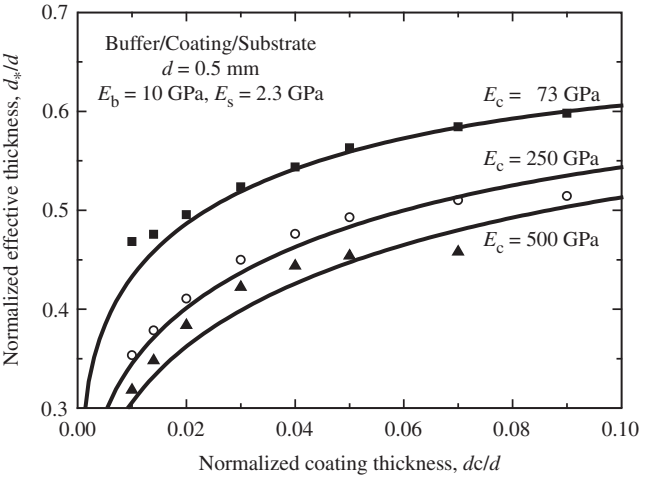

Figure 2. FEA data for d_*/d_i as a function of d_c/d for fixed $E_b = 10$ GPa and $E_s = 2.3$ GPa and selected values of E_c. The solid curves are for fits to equations (3)–(5).

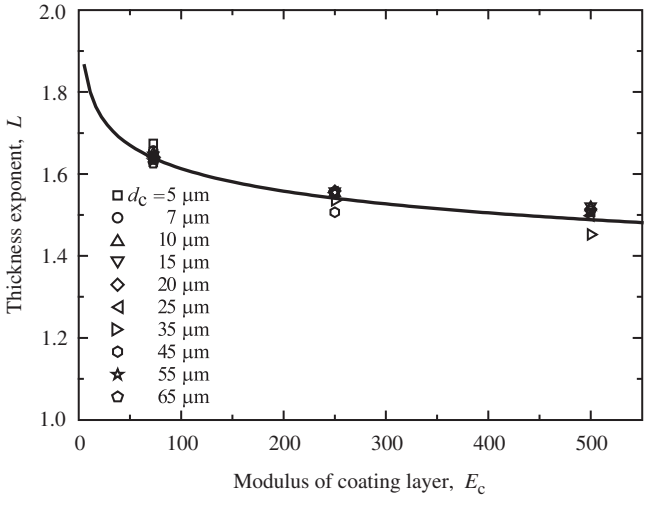

Figure 3. Plot for L as a function of E_c in equation (5), using FEA data from figure 2.

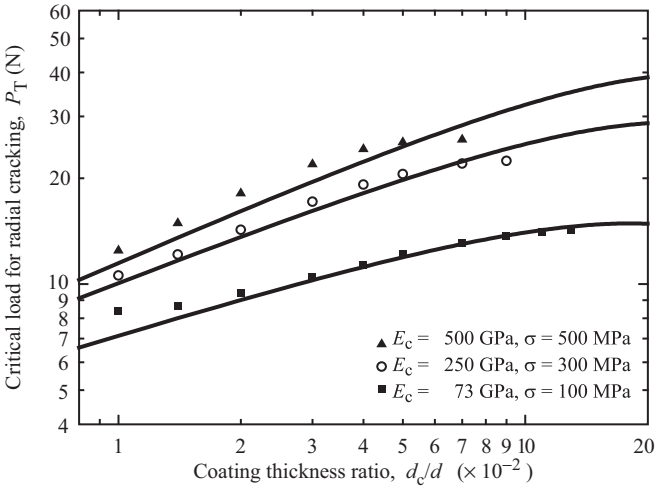

Figure 4. FEA data for P_T as a function of d_c/d for fixed $E_b = 10\,\text{GPa}$ and $E_s = 2.3\,\text{GPa}$ and selected values of E_c and σ. The solid curves are a regeneration from equation (6).

reaches the strength of coating layer. The equation for radial cracking can be derived under this assumption, and it can be written as:

$$P_T = \frac{B\sigma_F d_*^2}{\log(E_c/E_s)}. \tag{6}$$

Equation (6) has a simple form compared to equation (2) by replacing complicated correction factors B^*, C and E^* with d^*. Simultaneously, the critical load for radial

cracking P_T overcomes the limitation of P_R of bilayer systems. In figure 4, an analogous FEA result was replotted in terms of critical load for radial cracking. The strengths of the coating materials were assumed to be 100, 300 and 500 MPa. The trilayer equation mainly predicts the trends of the FEA results. A function fit of the critical load for the radial cracking and coating thickness ratios accommodate the determination of a single value strength for the brittle coating. In practical implementation, if the system is selected, the moduli and thicknesses of materials can be determined directly from the measurement and the indentation experiment gives the critical load for radial cracking. Finally, iterated calculation of experimental data set to equation (6) supplies the strength value for coating layer. Since this procedure can be conducted under the assumption of thin coated layer, the application of equation (6) should be restricted in thick coating.

3. Experiments

3.1. *Specimen preparation*

Two types of trilayer structures were prepared for a verification of the equation and for the case study. The trilayer structure consists of three layers; a buffer layer, a coating layer and a substrate. The buffer layer was prepared from a polished isotropic graphite plate with a lateral dimension of 20×20 mm (IG11; Toyo Tanso, Osaka, Japan); the substrate was prepared from polycarbonate slabs with an identical lateral dimensions and a 12.5 mm thickness. As a model trilayer system, a soda-lime glass plate (Menzel, Braunschweig, Germany) was utilized, as the physical properties of this type of glass are well-documented and it has been commonly used in similar, earlier studies. The glass undersurface was pre-abraded with grade 600 SiC grit to produce a uniform layer of initial surface flaws for the radial cracks. The total thickness of graphite and glass was fixed as 500 μm, and the thickness ratio of the coating of two layers was controlled to between 0.1 and 0.01. The graphite and glass plates were then bonded together and adhered to polycarbonate with epoxy glue.

Silicon carbide coating was used as a case study. Two grades of silicon carbide were deposited onto the graphite buffer layer. The polycrystalline silicon carbide films were deposited by a conventional hot-wall type low-pressure chemical vapour deposition system. The source gas was methyltrichlorosilane (MTS, CH_3SiCl_3), and hydrogen gas was used for dilution and for controlling the concentration of the source gas. MTS and H_2 were mixed with a ratio of 5 : 1, and the total flow rate was fixed at 800 sccm. The reaction chamber pressure was maintained at 20 T, and the deposition time was 1 h. To prepare different grades of SiC coatings, two deposition temperatures were selected: 1300 and 1350°C. The SiC film deposited at 1300°C showed a stratified microstructure, a preferred orientation of (111) and a small grain size (0.5–2 μm). In contrast, the SiC film deposited at 1350°C showed a faceted columnar microstructure with (220) preferred orientation and a comparatively large grain size (4–8 μm). The surface of the silicon carbide

was polished down to 1 μm diamond slurry to eliminate large starting flaws or defects. The polished silicon carbide deposited onto the graphite layer was bonded to the polycarbonate substrate, and the trilayer was prepared.

3.2. *Indentation testing*

Prior to the indentation testing experiments, the basic physical properties of each layer and adhesive were measured using several techniques. The Young's modulus of each layer was determined by an acoustic impulse excitation apparatus (Grindosonic, St. Louis, MO, USA) and a nanoindentor (Nanotester, MicroMaterials, Wrexham, UK). The strength of the abraded glass was measured by biaxial flexure test. The coating thicknesses of the glass and silicon carbide were measured with a high magnification optical microscope and observation with sliced samples. The microstructure and grain sizes of the silicon carbide were characterized with top views and side views taken by a scanning electron microscope. The preferred orientation of the silicon carbide was determined from X-ray diffractometry. The physical properties of the materials are summarized in table 1.

The top surface of the prepared trilayers was indented with a tungsten carbide sphere (radius 3.96 mm) mounted into the crosshead of a mechanical loading machine (Model 4400R; Instron, Canton, MA, USA). As the substrate and epoxy glue were transparent, the radial cracking of the coating layer was monitored from below using an aligned microscope zoom system (Zoom 100D; OPTEM, Santa Clara, CA, USA) coupled with a video camcorder. An *in situ* observation of radial cracks and loading data were recorded onto a digital video tape with a recorder and picture-in-picture apparatus, enabling a direct measurement of the critical load for the radial cracking, P_T. The data points from repeated testing on the trilayer structures were collected and used for fitting to equation (6) with the iterated calculation of the coating strength.

4. Results and discussion

The trilayer equation for radial cracking is derived from a modification of the bilayer and an introduction of the effective thickness concept. The trilayer critical load equation enables the measurement of the strength of the thin coating materials by

Table 1. Physical properties of materials.

Materials	Modulus E (GPa)	Hardness H (GPa)	Strength σ (MPa)
Graphite	10	–	–
Soda-lime glass	73	5.2	100
Polycarbonate	2.3	–	–
SiC (B)	215†	34†	991
Epoxy	3.5	–	–

†The values are determined by nanoindentation technique.

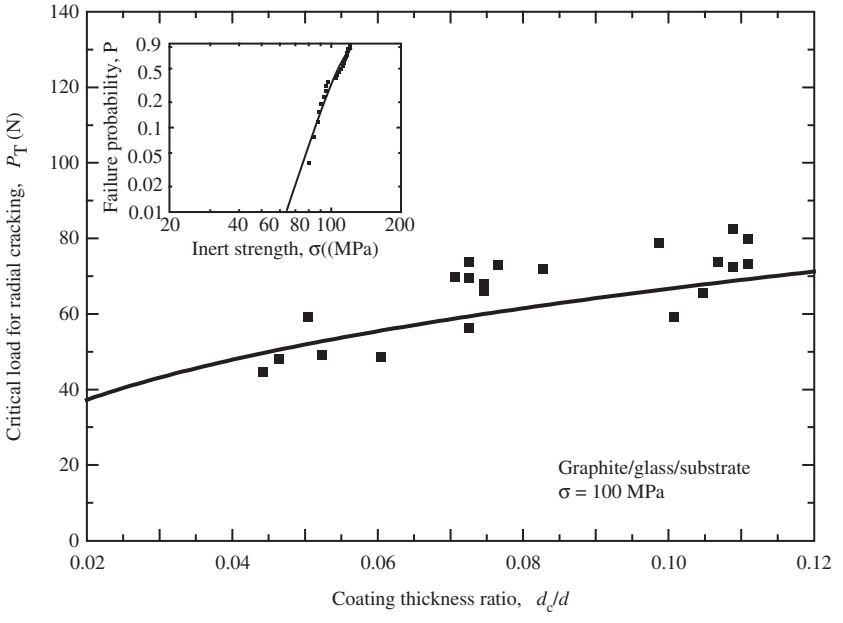

Figure 5. Experimental data showing the critical load P_T for radial cracking in graphite/glass/polycarbonate, as a function of the coating thickness ratio d_c/d. The solid curves are calculated from equation (5) with a glass strength value $\sigma = 100$ MPa. The inset shows the Weibull plot of glass.

adding a buffer layer onto the top of the coating layer, with a thickness ratio from 10 to 100. FEA assists the determination of an adjustable parameter in the trilayer equation. To confirm the validation of the suggested trilayer equation, a soda-lime glass with a strength of $\sigma = 100$ MPa was utilized as a model trilayer. In figure 5, the critical load for radial cracking in the soda-lime glass model trilayer system was measured and plotted as a function of the coating thickness ratio. In this plot, the solid curve was obtained by using the current trilayer equation. According to this result, the trilayer structure testing method was verified for brittle thin coating systems. In addition, the Weibull diagram included as an inset in figure 5, shows a linear fit to about 20 experimental strength values and yields a Weibull modulus of $m = 8.2$, which is a typical value for soda-lime glass. The small-scale materials had a size effect on the mechanical properties, as the size of the starting flaws was similar to the coating thicknesses. The coating thickness for the trilayer system was larger than 10 μm so that the effect of the flaw size in this experiment was not comparatively sensitive to the strength value. Care must be taken if extrapolating the trilayer equation for a very thin coating (<10 μm) or for a thick coating (>100 μm), as the size effect will appear in this testing range.

In this study, a trilayer equation was applied to compare two types of silicon carbide coatings. Two grades of SiC coating were fabricated (three different kinds of thicknesses, four specimens for each thickness), as shown in figure 6. As a result, two silicon carbide coatings with very different properties of grain size, microstructure

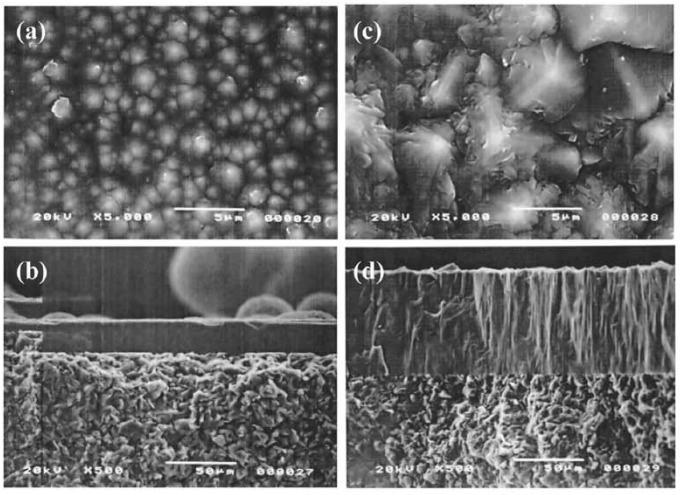

Figure 6. Microstructure of the deposited silicon carbide films (a) and (b) at 1300°C and (c) and (d) 1350°C, respectively, observed by a scanning electron microscope. Top views: (a) and (c); side views: (b) and (d).

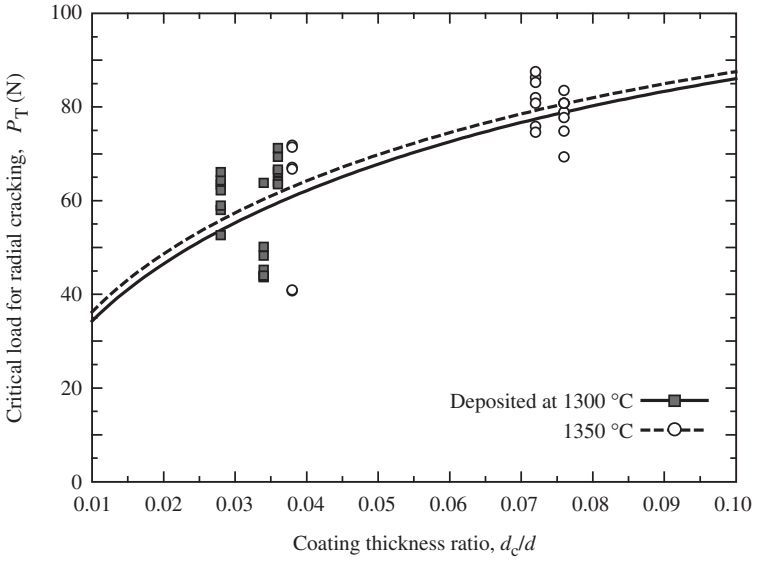

Figure 7. Experimental data showing the critical load for P_T for radial cracking in graphite/SiC/polycarbonate, as a function of the coating thickness d_c/d. The solid line (SiC(A)) and the dashed curve (SiC(B)) are fitted to the experimental results by adjusting the strength values.

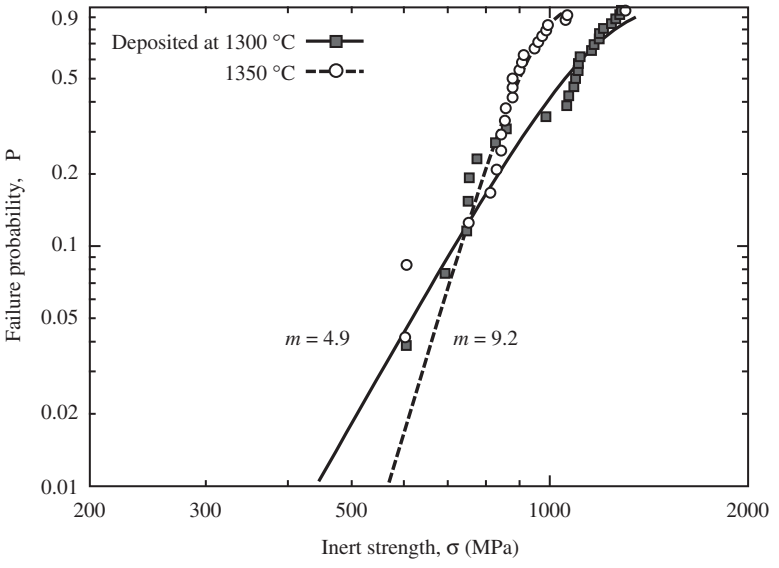

Figure 8. Weibull diagram for the silicon carbide films deposited at 1300°C (solid line) and 1350°C (dashed line), tested with the trilayer structure. The failure probability of the coatings was plotted as a function of the inert strength, and the *m* values indicate the Weibull modulus.

and preferred orientation (all caused by changing the deposition temperature) were obtained. The effects of temperature on the microstructure of the chemical vapour-deposited SiC are in good agreement with previous studies [17, 18]. The SiC (A) deposited at 1300°C exhibited a small thickness (<20 μm), while the SiC (B) deposited at 1350°C had a larger thickness of approximately 40 μm. Trilayer testing with the SiC coatings were performed for each thickness region with small variations. For a strength determination, a regression fit to the trilayer was conducted with all data points. In the case of this study, equation (6) can be reduced to simple polynomial function with the known values of thicknesses and moduli. The unknown value, strength, can be determined optimally with numerical calculations. This procedure yielded a single value for the strength of the coatings: the strength of the SiC (A) was 1053 MPa, while the strength of the SiC (B) was 991 MPa. Generally, in hard-coating systems, the isotropic microstructure shows a higher strength value than a columnar structure. In addition, small grain structure enhances the mechanical properties of coating, such as modulus, hardness and strength. The anisotropy of mechanical properties between SiC (A) and (B) can be inferred, connecting to the general trends.

The strength difference of the two SiC coatings was less than 100 MPa. Hence, there is no significant effect on the reliability of the coating systems. Based on the concept of the weakest link from the domain of extreme value statistics, the Weibull failure probability of the two SiC coatings plotted in figure 8. The linear fits are seen to be a reasonable representation of the data, showing each *m* value for the SiC coatings. The SiC (B) coatings have a large value for the Weibull modulus compared

to that of the SiC (A) coatings. From an engineering perspective, it is clear that the high Weibull modulus can be as important as the high strength or modulus. The SiC (A) show a high modulus and strength but is poor in terms of the failure probability characterization, while the SiC (B) shows a slightly smaller modulus and strength compared to the SiC (A) but a higher Weibull modulus. The linear fit of the SiC (A) shows a large deviation from a straight line. This fact reveals that the failure mode or flaw size distribution of the coating is not monotonic. The failure of a columnar structured SiC coating should be described by more appropriate functions. The major part of the testing of SiC coatings is the evaluation of the strength as well as the reliability. The trilayer testing results of SiC (A) and (B) has certain implications that materials selection for structural applications requires considering both the strength and the Weibull modulus.

5. Conclusion

From this result, it is concluded that trilayer testing can determine the strength of brittle thin films and is also useful for a comparison of the failure probabilities by combining the strength measurement and the Weibull plots. Trilayer testing method can be applied for the strength determination of most of the conventional coating system, including hard coatings, environmental barrier coatings and thermal barrier coatings in condition of $E_c > E_b > E_s$. In the trilayer testing method, a sample can be easily prepared by adhering a hard coating onto a transparent substrate and adding a buffer layer on the top coating surface. The strength of the coating can be determined by measuring the critical load for radial cracking via *in situ* observation technique. In addition, a sufficient number of strength data can be obtained from a small part of a sample, thus, it enables the statistical approach to the evaluation of the coating strength. The trilayer equation in this study can be taken as a useful testing technique for a characterization of the mechanical properties of brittle coating systems.

Acknowledgements

Thanks are due to Jong Hoon Park, Won Ju Kim, Ji Yeon Park and Young Woo Lee for their support with SiC coating fabrication and useful discussions. This work was supported by a grant from the Korea Atomic Energy Research Institute, through the Nuclear Hydrogen Development and Demonstration Program and by the Brain Korea 21 Program through Korean Ministry of Education.

References

[1] A.G. Evans, D.R. Mumm, J.W. Hutchinson, *et al.*, Prog. Mater. Sci. **46** 505 (2001).
[2] A. Arora and S.R. Parhakar, Mater. Technol. **18** 151 (2003).

[3] J.R. Kelly, J. Prosthet. Dent. **81** 652 (1999).
[4] C. Tang, Nucl. Eng. Des. **218** 91 (2002).
[5] W.J. Clegg, K. Kendall, N.M. Alford, *et al.*, Nature **347** 455 (1991).
[6] H. Chai, B.R. Lawn and S. Wuttiphan, J. Mater. Res. **14** 3805 (1999).
[7] E. Sanchez-Gonzalez, P. Miranda, A. Diaz-Parralejo, *et al.*, J. Mater. Res. **19** 896 (2004).
[8] P. Miranda, A. Pajares, F. Guiberteau, *et al.*, J. Mater. Res. **16** 115 (2001).
[9] J.H. Kim, P. Miranda, D.K. Kim, *et al.*, J. Mater. Res. **18** 222 (2003).
[10] H. Chai and B.R. Lawn, J. Mater. Res. **14** 3805 (1999).
[11] H. Chai and B.R. Lawn, J. Mater Res. **19** 1752 (2004).
[12] B.R. Lawn, Y. Deng, P. Miranda, *et al.*, J. Mater. Res. **17** 3019 (2002).
[13] Y. Deng, B.R. Lawn and I.K. Lloyd, J. Biomed. Mater. Res. **63** 137 (2002).
[14] T.J. Lardner, J.E. Ritter and G.-Q. Zhu, J. Am. Ceram. Soc. **80** 1851 (1997).
[15] S.J. Bull, D.G. Bhat and M.H. Statia, Surf. Coat. Technol. **163** 499 (2003).
[16] S.J. Yu, Z.F. Ding, J. Xu, *et al.*, Thin Solid Films. **390** 98 (2001).
[17] D.-J. Kim, D.-J. Choi and Y-W. Kim, Thin Solid Films **266** 192 (1995).
[18] H.-S. Kim and D.-J. Choi, Thin Solid Films **312** 195 (1998).
[19] D.P. Stinton, T.M. Besmann and R.A. Rowden, Ceram. Bull. **67** 350 (1988).
[20] E. Minford, R.E. Stevens, V.L. Magnooa, *et al.*, Mater. Res. Soc. Symp. Proc. **168** 223 (1989).
[21] C.A. Brookes, Nature **228** 660 (1970).